

## Supporting Information

### **Time-correlated single-photon counting investigation of the photophysical properties of poly(paraphenylene) (PPP) and poly(fluorene) (PF).**

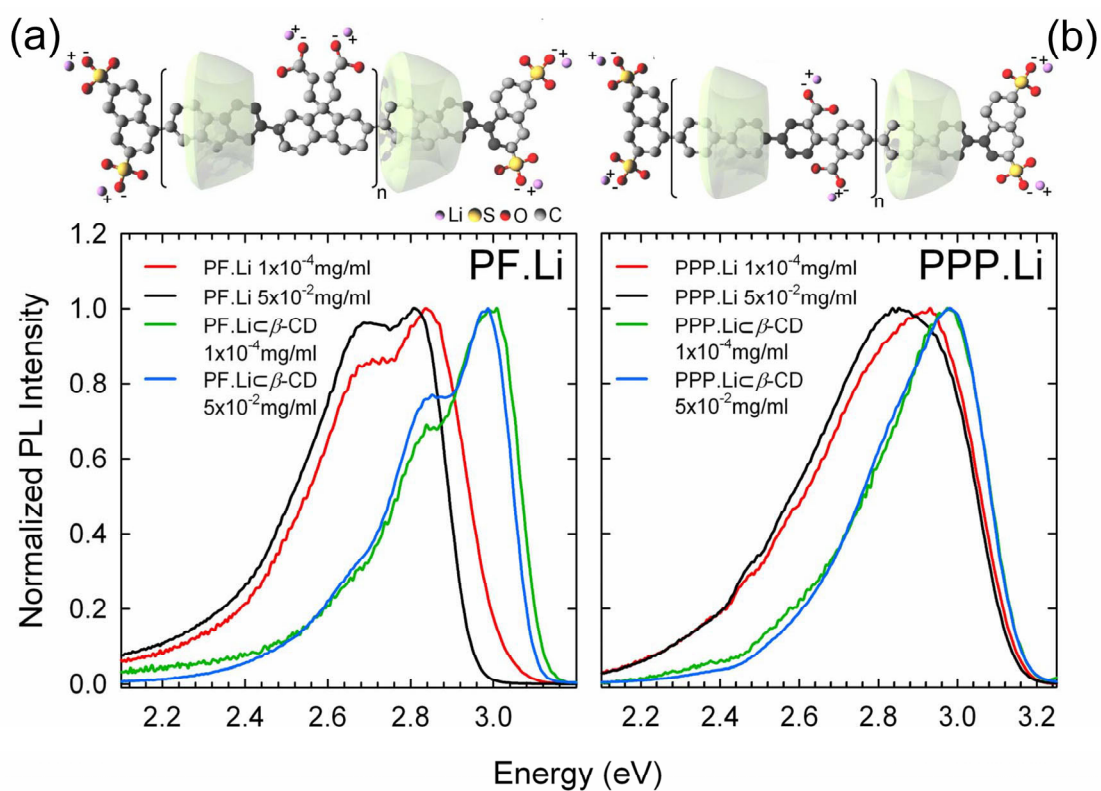
We have also characterized the solution photophysics of unthreaded and rotaxinated poly(fluorene) (PF) and poly(paraphenylene) (PPP), with results similar to those found for PDV. Steady state and time-resolved PL measurements were carried out on buffer solutions at the same concentrations used for PDV.Li, namely  $5 \times 10^{-2}$ ,  $1 \times 10^{-3}$  and  $1 \times 10^{-4}$  mg/ml. The experiments were performed in the same experimental conditions. The results reported in the supplementary figures below show that the photophysical properties of both PF.Li- $\beta$ -CD and PPP.Li- $\beta$ -CD are independent of concentration, in agreement with what observed for PDV-based polyrotaxanes.

**We conclude that cyclodextrin encapsulation is a successful and general strategy for suppressing the interchain interactions in all the investigated materials.**

## Supplementary Figures

### Supplementary Fig. 1: Time-integrated fluorescence spectral properties of CD-threaded and unthreaded PPP and PF

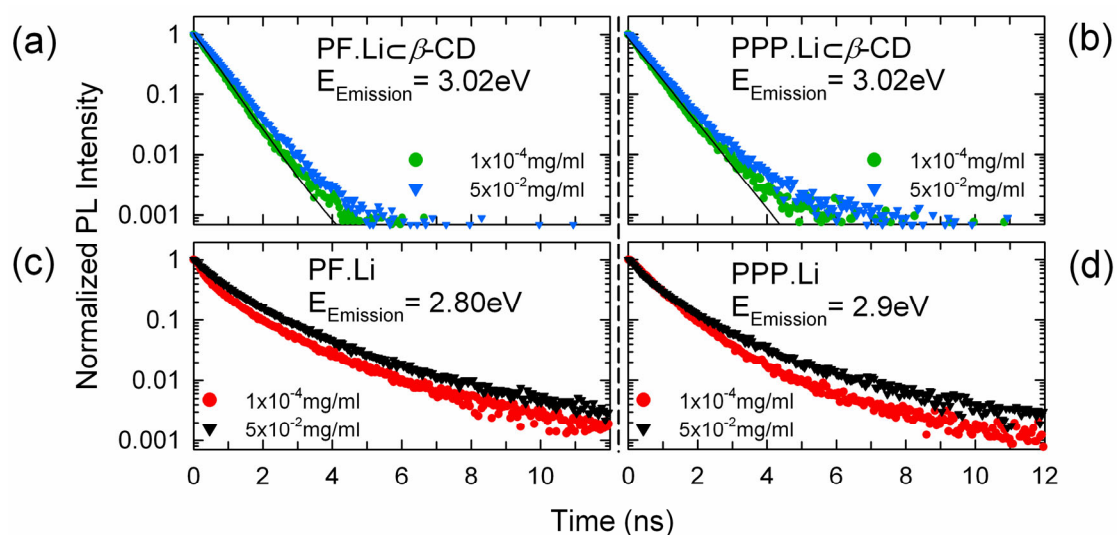
The fluorescence spectral profiles of unthreaded and rotaxinated PF.Li (Supplementary Figure. 1a) and PPP.Li (Supplementary Figure. 1b) are reported in Supplementary figure 1. In agreement with the results on PDV.Li $\subset\beta$ -CD, the PL spectra of PF.Li $\subset\beta$ -CD and PPP.Li $\subset\beta$ -CD are independent of concentration. We observe that the PL spectra of the lowest concentrated solution of unthreaded PPP.Li evolves from substantially matching the emission profile of the rotaxinated analogues by exhibiting a red-shift of about 200 meV in the highest concentration case (Supplementary Figure. 1b). The effect of interchain interactions is less pronounced for unthreaded PPP.Li than for unthreaded PF.Li, whose PL spectra in solution are significantly red-shifted (more than 300 meV) with respect to the polyrotaxanes ones. This is likely to be due to a larger dihedral angle between the monomeric units of PPP.Li, compared to PF.Li.



**Supplementary Fig. 1: Time-integrated fluorescence spectral properties.** Time-integrated emission spectra of (a) Poly(fluorene) (PF) and PF.Li- $\beta$ -CD solutions at  $5 \times 10^{-2}$  mg/ml  $1 \times 10^{-4}$  mg/ml and (b) unthreaded poly(paraphenylene) and PPP.Li- $\beta$ -CD at the same concentrations as in panel (a). Excitation is at 3.3 eV for all spectra.

## Supplementary Fig. 2: Photoluminescence decay curves of CD-threaded and unthreaded PPP and PF

Supplementary Fig. 2 shows the PL decay curves for buffer solutions of the investigated materials at increasing concentration. The decay kinetics of both polyrotaxanes follows a single exponential law (for about 3 decades for PF.Li $\subset\beta$ -CD and about two decades for PPP.Li $\subset\beta$ -CD). A single-exponential fit of the decay curves of polyrotaxanes solutions yields decay rate values ( $k_{\text{PF.Li}}=1.89\times 10^9 \text{ s}^{-1}$ ) and ( $k_{\text{PPP.Li}}=1.81\times 10^9 \text{ s}^{-1}$ ), corresponding to experimental fluorescence lifetimes of 540 ps and 550 ps for PF.Li and PPP.Li, respectively. As observed for unthreaded PDV.Li, the deexcitation kinetics for both unthreaded PF.Li and PPP.Li is poly-exponential. Looking at the decay curves of unthreaded PPP.Li and PF.Li, we notice that the difference in the decay kinetics between the lowest and the highest concentrated solutions is more pronounced for the PPP.Li than for the PF.Li solutions. Furthermore, the PL decay curves of unthreaded PPP.Li and PF.Li do not follow a single-exponential law even at a concentration of  $1\times 10^{-4}$  mg/ml. We ascribe this effect to the decreasing solubility ( $\zeta$ ) in aqueous solvents,  $\zeta_{\text{PDV.Li}} > \zeta_{\text{PPP.Li}} > \zeta_{\text{PF.Li}}$ , as a result of the higher hydrophobic character of PF.Li and PPP.Li compared to PDV.Li, which may favour hydrophobic binding among the conjugated moieties and the phase separation of the aromatic systems in low-polarity domains. In this pseudo-colloidal condition, in which the main interactions are polymer-polymer instead of polymer-solvent, the formation of interchain species is clearly favored.



**Supplementary Fig. 2:** Time-dependent decays of solutions of (a) PF.Li $\beta$ -CD and (b) PPP.Li $\beta$ -CD at 3.02 eV, and of the unthreaded polymers (c) PF.Li at 2.80 eV and (d) PPP.Li at 2.9 eV. The relative fits are also shown for the polyrotaxane decays, which have been fitted by a simple exponential function. Excitation is at 3.3 eV in all cases.

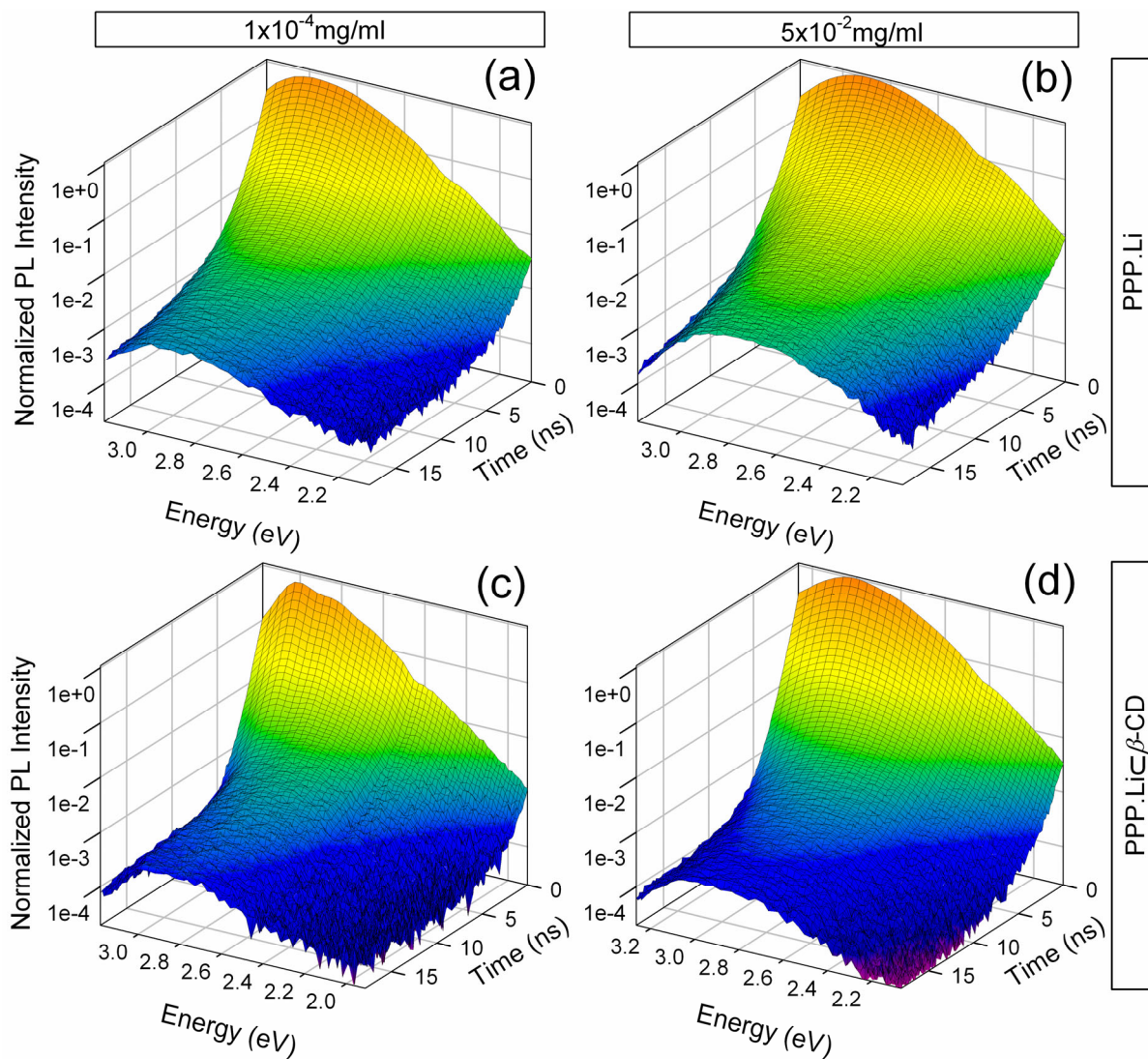
**Supplementary Fig. 3: Time-resolved fluorescence of CD-threaded and unthreaded PPP**

**Supplementary Fig. 4: Time-resolved fluorescence of CD-threaded and unthreaded PF**

Finally we report the 3D plots of PL time decay as a function of emission energy for the least and most concentrated solutions of unthreaded and rotaxinated PPP.Li (Supplementary Fig. 3) and PF.Li polymers (Supplementary Fig. 4), respectively.

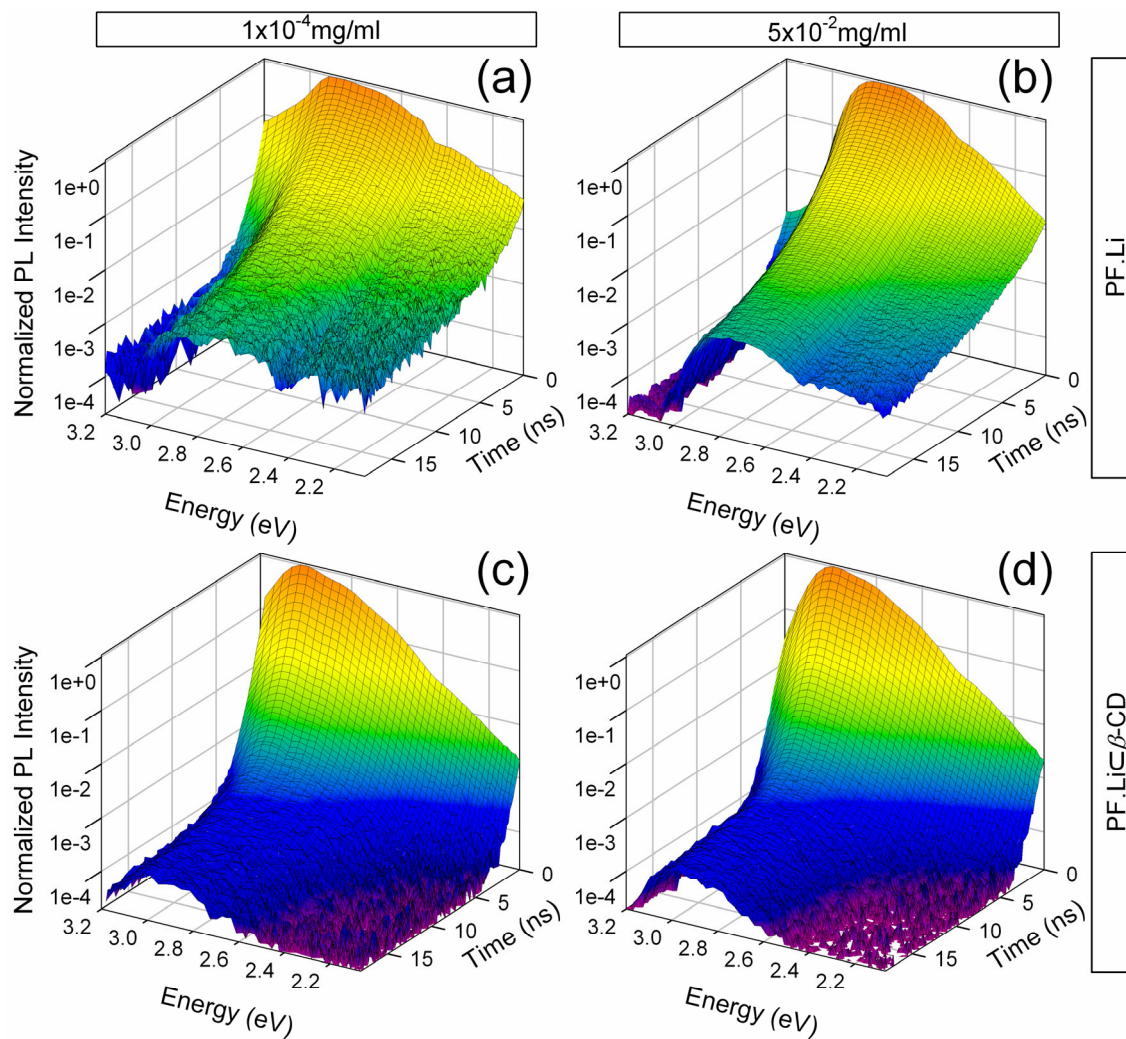
Looking at the dynamics of unthreaded PPP.Li (Supplementary Fig. 3a, b), we notice that the PL profile of the least concentrated solutions is centred at higher energy with respect to the high concentration case. The spectral shape of the most diluted solution is conserved during the decay, as we note from the PL spectrum at about 20 ns after the excitation pulse (Supplementary Fig. 3a). On the contrary, the PL arising from the most concentrated solution clearly exhibits two distinct spectral features: a fast initial decay at about 3 eV followed by a long lived tail at lower energy ( $\sim 2.9$  eV). Similar behaviour is observed for PF.Li, where a strong quenching of the fast component at 3.1 eV is even more evident (Supplementary Fig. 4a, b) as the concentration is increased.

As for the case of PDV.Li, we interpret the fast blue emission as a contribution from the decay of intramolecular excitons and the slow red-shifted band as the contribution of interchain species. The time evolution of the PL spectra of rotaxinated PPP.Li and PF.Li solutions (Supplementary Fig. 3c, d) and Supplementary Fig. 4c, d) is instead dominated by the intramolecular exciton emission (centred at about 3 eV), in agreement with the PDV.Li results.



**Supplementary Fig. 3: Time-resolved fluorescence.**

3D plot of PL time decay excited at 3.3eV as a function of emission energy for the least ( $1 \times 10^{-4}$  mg/ml) (a,c) and most concentrated ( $5 \times 10^{-2}$  mg/ml) (b,d) solutions of unthreaded PPP.Li and PPP.Li@ $\beta$ -CD polymer, respectively.



**Supplementary Fig. 4: Time-resolved fluorescence.**

3D plot of PL time decay excited at 3.3eV as a function of emission energy for the least ( $1 \times 10^{-4} \text{ mg/ml}$ ) (a,c) and most concentrated ( $5 \times 10^{-2} \text{ mg/ml}$ ) (b,d) solutions of unthreaded and rotaxinated PF.Li polymer, respectively.